

Observational Study

Nomogram based on liver stiffness and spleen area with ultrasound for posthepatectomy liver failure: A multicenter study

Guang-Wen Cheng, Yan Fang, Li-Yun Xue, Yan Zhang, Xiao-Yan Xie, Xiao-Hui Qiao, Xue-Qi Li, Jia Guo, Hong Ding

Specialty type: Gastroenterology and hepatology

Provenance and peer review:

Unsolicited article; Externally peer reviewed.

Peer-review model: Single blind

Peer-review report's classification

Scientific Quality: Grade B, Grade B, Grade C

Novelty: Grade B, Grade B, Grade C

Creativity or Innovation: Grade B, Grade B, Grade C

Scientific Significance: Grade B, Grade B, Grade C

P-Reviewer: Hernandez-Munoz R; Lampri E; Sivapatham S

Received: February 28, 2024

Revised: May 24, 2024

Accepted: June 17, 2024

Published online: July 21, 2024

Processing time: 133 Days and 15 Hours



Guang-Wen Cheng, Yan Fang, Li-Yun Xue, Xiao-Hui Qiao, Xue-Qi Li, Department of Ultrasound, Huashan Hospital, Fudan University, Shanghai 200040, China

Yan Zhang, Jia Guo, Department of Ultrasound, Shuguang Hospital Affiliated to Shanghai University of Traditional Chinese Medicine, Shanghai 201203, China

Xiao-Yan Xie, Department of Medical Ultrasonics, Institute of Diagnostic and Interventional Ultrasound, Sun Yat-sen University First Affiliated Hospital, Guangzhou 510080, Guangdong Province, China

Xue-Qi Li, Institute of Ultrasound in Medicine and Engineering, Shanghai Cancer Center, Shanghai 200040, China

Jia Guo, Department of Ultrasound, Eastern Hepatobiliary Surgical Hospital, Second Military Medical University, Shanghai 200433, China

Hong Ding, Department of Ultrasound, National Clinical Research Center for Aging and Medicine, Huashan Hospital, Fudan University, Shanghai 200040, China

Co-first authors: Guang-Wen Cheng and Yan Fang.

Co-corresponding authors: Jia Guo and Hong Ding.

Corresponding author: Hong Ding, MD, PhD, Professor, Department of Ultrasound, Huashan Hospital, Fudan University, No. 12 Urumqi Middle Road, Shanghai 200040, China.

ding_hong@fudan.edu.cn

Abstract

BACKGROUND

Liver stiffness (LS) measurement with two-dimensional shear wave elastography (2D-SWE) correlates with the degree of liver fibrosis and thus indirectly reflects liver function reserve. The size of the spleen increases due to tissue proliferation, fibrosis, and portal vein congestion, which can indirectly reflect the situation of liver fibrosis/cirrhosis. It was reported that the size of the spleen was related to posthepatectomy liver failure (PHLF). So far, there has been no study combining 2D-SWE measurements of LS with spleen size to predict PHLF. This prospective study aimed to investigate the utility of 2D-SWE assessing LS and spleen area

(SPA) for the prediction of PHLF in hepatocellular carcinoma (HCC) patients and to develop a risk prediction model.

AIM

To investigate the utility of 2D-SWE assessing LS and SPA for the prediction of PHLF in HCC patients and to develop a risk prediction model.

METHODS

This was a multicenter observational study prospectively analyzing patients who underwent hepatectomy from October 2020 to March 2022. Within 1 wk before partial hepatectomy, ultrasound examination was performed to measure LS and SPA, and blood was drawn to evaluate the patient's liver function and other conditions. Least absolute shrinkage and selection operator logistic regression and multivariate logistic regression analysis was applied to identify independent predictors of PHLF and develop a nomogram. Nomogram performance was validated further. The diagnostic performance of the nomogram was evaluated with receiver operating characteristic curve compared with the conventional models, including the model for end-stage liver disease (MELD) score and the albumin-bilirubin (ALBI) score.

RESULTS

A total of 562 HCC patients undergoing hepatectomy (500 in the training cohort and 62 in the validation cohort) were enrolled in this study. The independent predictors of PHLF were LS, SPA, range of resection, blood loss, international normalized ratio, and total bilirubin. Better diagnostic performance of the nomogram was obtained in the training [area under receiver operating characteristic curve (AUC): 0.833; 95% confidence interval (95% CI): 0.792-0.873; sensitivity: 83.1%; specificity: 73.5%] and validation (AUC: 0.802; 95% CI: 0.684-0.920; sensitivity: 95.5%; specificity: 52.5%) cohorts compared with the MELD score and the ALBI score.

CONCLUSION

This PHLF nomogram, mainly based on LS by 2D-SWE and SPA, was useful in predicting PHLF in HCC patients and presented better than MELD score and ALBI score.

Key Words: Shear-wave elastography; Spleen; Hepatectomy; Posthepatectomy liver failure; Hepatocellular carcinoma

©The Author(s) 2024. Published by Baishideng Publishing Group Inc. All rights reserved.

Core Tip: Posthepatectomy liver failure (PHLF) is a major complication after hepatectomy. Liver stiffness (LS) measured by ultrasound elastography can reflect liver reserve function, while splenic enlargement can also reflect liver reserve function. Ultrasound measurement of splenic size is simple, but there were few studies that used splenic size to predict PHLF. Our study used ultrasound elastography combined with spleen size and serological indicators to establish a predictive model for PHLF. It had the potential to predict PHLF, indicating that LS, and spleen size could be used for risk stratification in patients.

Citation: Cheng GW, Fang Y, Xue LY, Zhang Y, Xie XY, Qiao XH, Li XQ, Guo J, Ding H. Nomogram based on liver stiffness and spleen area with ultrasound for posthepatectomy liver failure: A multicenter study. *World J Gastroenterol* 2024; 30(27): 3314-3325

URL: <https://www.wjgnet.com/1007-9327/full/v30/i27/3314.htm>

DOI: <https://dx.doi.org/10.3748/wjg.v30.i27.3314>

INTRODUCTION

Hepatocellular carcinoma (HCC) is the most common malignant liver tumor and the third-leading cause of cancer deaths worldwide[1]. Currently, surgical resection remains the preferred effective treatment for HCC. However, posthepatectomy liver failure (PHLF) is a major complication after hepatectomy, with a reported incidence ranging from 0.7% to 39.6%[2,3]. PHLF is a major cause of death in patients after hepatectomy with an approximate 50% mortality rate[4]. Therefore, an accurate risk prediction of PHLF is essential for improving clinical treatment strategies for HCC patients. The occurrence of PHLF is not only related to the scope of liver resection but also closely related to the liver reserve function of the residual liver. The presence of liver fibrosis or cirrhosis in over 70%-90% of HCC patients[5] has a significant impact on liver reserve function. Therefore, a comprehensive and effective preoperative evaluation of liver reserve function is crucial for developing a reasonable surgical plan to reduce the occurrence of PHLF.

The indocyanine green clearance test is widely used in Asia to evaluate liver reserve function. However, the accuracy of the results of this method may be influenced by multiple factors, so its effectiveness in predicting PHLF has been unsatisfactory in multiple studies[6-8]. In addition, some clinical models for assessing liver function reserve, such as the laboratory index-based model for end-stage liver disease (MELD) score and albumin-bilirubin (ALBI) score, have proven

to be of certain value in predicting the PHLF risk, but the predictive accuracy of these models remains inadequate with a ceiling effect[9,10]. Therefore, these methods have not been included in the current international HCC management guidelines and are not routinely used worldwide.

Computed tomography has been used to measure residual liver volume to predict PHLF in patients scheduled for major liver resection. However, residual liver volume cannot fully represent liver reserve function, especially for patients with liver cirrhosis[6]. Gadolinium ethoxybenzyl diethylenetriamine pentaacetic acid directly measures liver reserve function. However, this method is expensive and time-consuming, and previous reports have shown that its application requires complex calculations[11,12].

Liver stiffness (LS) measurement with two-dimensional shear wave elastography (2D-SWE) correlates with the degree of liver fibrosis and thus indirectly reflects liver function reserve[13-15]. Several previous studies showed a good predictive value of 2D-SWE for PHLF[6,16-18]. However, these studies investigated a small number of cases and lacked external validation. In addition, there was a deviation in LS measurements by ultrasound elastography during liver inflammation[19]. Splenomegaly is common in patients with liver fibrosis, especially cirrhosis. Due to the close correlation between liver fibrosis/cirrhosis and portal hypertension, as portal hypertension progresses, spleen size increases due to tissue proliferation, fibrosis, and portal vein congestion, which can indirectly reflect the situation of liver fibrosis/cirrhosis. Spleen size has been reported to be associated with PHLF[20,21]. So far, there have been no studies to predict PHLF by combining 2D-SWE measurement of LS with spleen size.

Therefore, the aim of the present study was to develop and validate a comprehensive PHLF prediction model based on LS measurement by 2D-SWE, spleen size, surgical factors, and laboratory indexes for providing better risk stratification of HCC patients before hepatectomy.

MATERIALS AND METHODS

Study design and population

This was a multicenter observational study consisting of two cohorts, a training cohort and a validation cohort. Between October 2019 and March 2022, consecutive patients undergoing hepatectomy were prospectively enrolled from centers A (Huashan Hospital), B (Eastern Hepatobiliary Surgical Hospital), and C (Shanghai Cancer Center) as the training cohort. Patients from centers D (Shuguang Hospital Affiliated to Shanghai University of Traditional Chinese Medicine) and E (Sun Yat-sen University First Affiliated Hospital) were enrolled as the validation cohort. The inclusion criteria were as follows: (1) Age between 18 years and 85 years; (2) Patients with liver tumors prepared for partial hepatectomy; (3) Liver function classification of Child-Pugh A, B, or C; (4) Eastern Cooperative Oncology Group performance score 0-2[22]; and (5) LS measurement by 2D-SWE and spleen examination by ultrasound within 1 wk prior to surgery. The exclusion criteria were as follows: (1) Postoperative pathology indicating non-HCC; (2) Patients receiving preoperative anticancer treatment such as transhepatic arterial chemotherapy and embolization; (3) Patients receiving intraoperative ablation; (4) History of previous liver resection; (5) Failure in LS; and (6) Missing data. The detailed flowchart of patient selection is shown in [Figure 1](#).

Data collection

The following patient data were collected: Demographic data (age and sex); preoperative laboratory data, including total bilirubin (TB), albumin, alanine transaminase, prothrombin time, international normalized ratio (INR), platelet (PLT) count, γ -glutamyl transpeptidase, white blood cell count, hemoglobin, alpha-fetoprotein, hepatitis B virus (HBV) status, and HBV-DNA level; tumor-related data (tumor size and number); surgical data [hepatic portal clamping time, blood loss (BL)]; liver resection range (RR) (major hepatectomy defined as liver resection of ≥ 3 Couinaud segments, minor hepatectomy defined as liver resection of < 3 Couinaud segments)[23]; and information about ultrasound imaging examination (LS measurement and spleen measurement).

Examination and interpretation of LS measurement by 2D-SWE

Liver 2D-SWE examination was performed on all patients using the Aixplorer ultrasound imaging system (Supersonic Imagine, Aix-en-Provence, France) equipped with a convex array probe SC6-1. In accordance with the European Federation of Societies for Ultrasound in Medicine and Biology guidelines, the procedures for liver 2D-SWE examination were as follows. The patient was asked to lie in a supine position with the right arm above the head after at least 4 h of fasting. An appropriate right intercostal or subcostal space was located for observing the right liver parenchyma using gray-scale ultrasound imaging; subsequently, the SWE model was switched on for elastography. The patient was then instructed to hold breath for at least 5 s to obtain a stabilized SWE image, and meanwhile the sampling frame (approximately 4 cm \times 3 cm) was placed vertically on the liver parenchyma 1-2 cm below the liver capsule and at least 2 cm from the margins of liver masses, avoiding the intrahepatic vessels and bile duct. The color-coded elasticity map was required more than 80% filled. A region of interest (2 cm in diameter) was placed at the sampling frame for stiffness measurement in kPa. Five independent measurements were performed, and the measurements were considered successful when the interquartile range/median value was below 30%. Ultimately, the median of the five measurements was used as LS measurement.

Examination and interpretation of spleen area by ultrasound.

The longitudinal view of the spleen with the hilus was observed through the intercostal space near the tenth rib from the

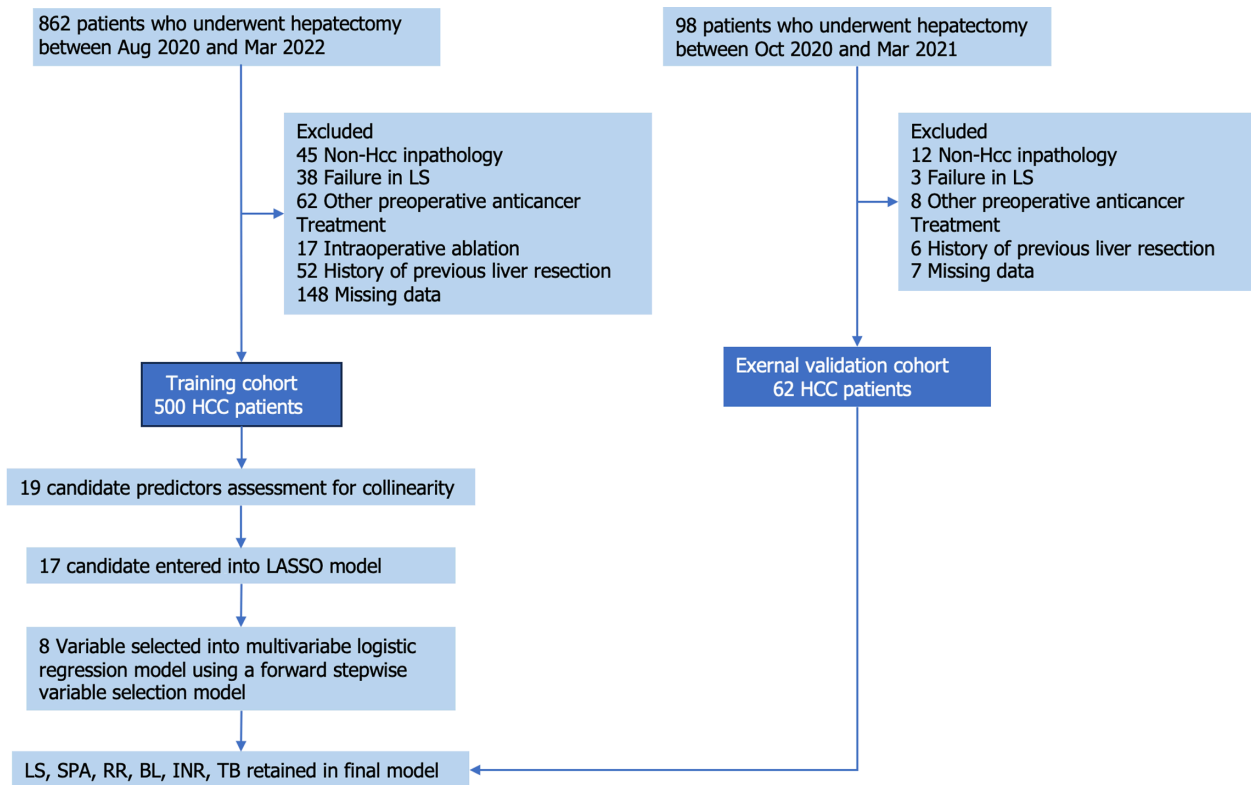


Figure 1 Flow chart of the cohorts in the study. BL: Blood loss; HCC: Hepatocellular carcinoma; INR: International normalized ratio; LASSO: Least absolute shrinkage and selection operator; LS: Liver stiffness RR: Resection range; SPA: Spleen area; TB: Total bilirubin.

posterior axillary line when the patient was placed in the right lateral position. In this location, the length and width of the spleen were measured. The spleen area (SPA, cm²) was defined as the length (cm) × width (cm).

Diagnosis and definition

PHLF was diagnosed according to the criteria of the International Study Group on Liver Surgery[24]: According to the upper limit of normal values of the local laboratory on postoperative day 5, an increase in the INR (> 1.2) and hyperbilirubinemia (> 22 μmol/L or above preoperative value). The severity of PHLF was divided into three categories based on clinical management: Grade A, which does not require further clinical management; grade B, which requires active therapeutic intervention without invasive approaches; and grade C, which requires an invasive approach. We defined grade B and C PHLF as symptomatic PHLF (SPHLF), grade A or no PHLF were defined as non-SPHLF[25].

Statistical analysis

According to the sample size estimation of the area under receiver operating characteristic curve (AUC) of the diagnostic test and the incidence of PHLF in the literature, when the sensitivity = 0.90, the sample size was calculated for the diagnostic efficiency. AUC = 0.95, significance level = 0.05, power = 0.90, and the required sample size was calculated as 167 cases. A total sample size of 334 cases was required for the two subgroups.

Continuous variables in normal distribution were displayed as mean ± SD and analyzed by Student's *t* test, while continuous variables in non-normal distribution were presented as median (interquartile range) and analyzed by Mann-Whitney *U* test. In addition, categorical variables expressed as frequency (percentage) were compared by Pearson's χ^2 test or Fisher's exact test.

In the training cohort, the least absolute shrinkage and selection operator regression method was used to reduce the candidate predictor variables. We used logistic regression to further screen independent predictors and establish a multivariate prediction model. In this process, we used the stepwise forward method in SPSS to screen variables in the logistic regression model and used the default *P* = 0.1 in SPSS to determine the independent variables included in the model. A nomogram based on the predictive model was constructed and further validated in the validation cohort.

The AUC was used to assess the diagnostic performance of the predictive model compared with other traditional models (MELD score and ALBI score), and the AUC values were compared by DeLong's tests. Bootstrap with 2000 resampling was generated for the calibration curve in the training and validation cohorts as internal and external validation. The decision curve analysis (DCA) was used to evaluate the clinical effectiveness of the prediction model. *P* < 0.05 indicated a statistically significant difference. All the above statistical analyses were performed in R software (v.4.1.0; <http://www.r-project.org/>) and SPSS (version 20.0; IBM Corp., Armonk, NY, United States).

RESULTS

Clinical features

The study included 500 eligible participants in the training cohort and 62 in the validation cohort. There were 142 cases and 22 cases of PHLF in the training cohort and the validation cohort, respectively. Among them, the number of PHLF A, PHLF B and PHLF C cases were 106, 32, and 4 cases in the training cohort, and 15, 6, and 1 cases in the validation cohort, respectively. One patient in the training cohort died within 90 d after surgery, with a mortality rate of 0.2%. The baseline characteristics of the patients are listed in [Table 1](#). The baseline clinicopathologic data, including sex, age, laboratory indexes such as TB, INR, PLT, alpha-fetoprotein, HBV status, and HBV-DNA, tumor-related data, and surgical data such as BL, RR, LS, and SPA did not show significant differences between the training and validation cohorts ($P > 0.05$).

Selection of predictors and construction of nomogram model

Least absolute shrinkage and selection operator regression of the training cohort showed the right clinical and ultrasound features with non-zero coefficients with a minimum lambda value of 0.06. These features included the following eight variables: LS; SPA; RR; BL; alanine transaminase; prothrombin time; INR; and TB. Based on the above-screened variables, logistic regression was used to construct a multivariate prediction PHLF model (PM), which ultimately included six variables shown in [Figure 2](#). Based on the multivariate prediction model, we developed a PM nomogram ([Figure 3](#)) to predict the risk of PHLF to provide a quantitative method for the clinicians. The score and predicted probability of PHLF can be calculated using the following formulas: $PM = -8.343 + 0.176 \times LS + 0.082 \times SPA + 0.001 \times BL - 1.086 \times RR$ (major = 1; minor = 0) + $0.049TB + 0.148 \times INR$ (multiplied by 10). The predicted probability of PHLF = $1/[1 + \exp(-PM + 8.298)]$.

Diagnostic performance of the PM compared with previously reported models

In order to confirm the clinical utility of PM, we analyzed the correlation between the PM model and the previous commonly used ALBI and MELD models, and the spearman correlation coefficients between PM and ALBI and MELD were 0.62 and 0.59, respectively (both $P < 0.05$). The receiver operating characteristic curve and AUC values of the PM and the previously reported models (ALBI score and MELD score) for estimating PHLF risk were calculated and compared in the training and validation cohorts ([Figure 4](#), [Table 2](#)). In both the training and validation cohorts, the predictive performance of PM on PHLF were significantly higher than those of ALBI and MELD ($P < 0.05$).

Calibration and DCA

The calibration curves (2000 bootstrap resamples) are graphically shown for the validation of the PM in both cohorts ([Figure 5](#)). The Hosmer-Lemeshow tests exhibited $P = 0.752$ in the validation cohort, which suggested that the predicted probability of the PM was well consistent with the actual outcome. The DCA curve also indicated that the PM had good clinical utility.

Subgroup analysis of SPHLF and non-SPHLF

The median LS of the SPHLF group was significantly higher than that of the non-SPHLF group (14.50 kPa *vs* 13.34 kPa, $P = 0.048$). Multivariate logistic regression analysis showed that LS ($P < 0.05$) and major liver resection ($P < 0.001$) were the independent predictors of SPHLF. Namely, patients with $LS \geq 12.52$ kPa have an increased risk of SPHLF (odds ratio: 1.28), at which point the AUC of LS diagnosis of SPHLF is 0.80. Among all patients with PHLF, the incidence of SPHLF was significantly higher in patients with major liver resection than in those with minor liver resection (51.2% *vs* 14.1%, $P < 0.001$).

Subgroup analysis of the major liver resection group and the minor liver resection group using dual cutoff diagnosis based on LS and SPA

In patients with PHLF, the LS value and SPA in the major liver resection group were significantly lower than those in the minor liver resection group (LS: 13.00 kPa *vs* 14.24 kPa; $P = 0.046$; SPA: 45.3 cm² *vs* 53.8 cm²; $P = 0.0013$). The diagnostic cutoff values of LS and SPA in 2D-SWE for diagnosing PHLF in the major liver resection and minor liver resection groups were evaluated using the dual cutoff diagnosis: For LS, 10.34 kPa in the major liver resection group (AUC = 0.74) and 13.48 kPa in the minor liver resection group (AUC = 0.78); and for SPA: 33.7 cm² in the major liver resection group (AUC = 0.78) and 43.2 cm² in the minor liver resection group (AUC = 0.84).

DISCUSSION

It is clinically important to assess preoperative liver function reserve to predict the development of PHLF. Our model comprehensively considered the effects of preoperative liver status and intraoperative factors. Multiple variable screening methods were used, combined with ultrasound indicators, serological indicators, and surgical-related indicators, to comprehensively evaluate the impact of relevant factors on the occurrence of PHLF. Through the nomogram, the contribution of various predictive indicators in the PM was visually displayed.

INR, TB, RR, and BL are all independent risk factors for PHLF. This is reasonable because INR and TB are the recognized indicators that reflect PHLF and are used to develop PHLF prediction models[9]. As for the RR, a high volume of hepatectomy is related to increased risks of PHLF[26]. BL is also an independent risk factor for PHLF, which is consistent with the study by Fang *et al*[27] Considering that the liver is a blood-rich organ, excessive bleeding may

Table 1 Descriptive characteristics of the study population, *n* (%)

Characteristics	Training cohort	Validation cohort	<i>P</i> value
Patients	500	62	
PHLF	142 (28.40)	22 (35.50)	0.250
Sex			0.080
Male	413 (89.01)	45 (72.58)	
Female	87 (10.99)	17 (27.42)	
Age in yr, mean ± SD	55.70 ± 10.70	53.05 ± 10.62	0.067
TB in mg/dL, median; IQR	12.8; 9.9-17.0	13.4; 9.2-17.2	0.740
ALB in g/L, median; IQR	43; 40.0-46.0	41; 38.8-45.0	0.130
ALT in U/L, median; IQR	27; 19.0-38.0	32; 21.0-39.0	0.250
PT in s, median; IQR	12.4; 11.7-13.2	12.0; 11.5-13.0	0.080
INR, median; IQR	10.5; 9.9-11.1	10.2; 9.7-10.9	0.110
PLT as × 10 ⁹ /L, median; IQR	148.5; 111.0-197.0	167.5; 139.8-192.0	0.060
GGT in U/L, median; IQR	43.0; 11.0-1019.0	44.5; 16.0-543.0	0.190
WBC as × 10 ⁹ , median; IQR	5.55; 1.84-14.07	5.88; 2.01-14.30	0.250
HB in g/L, median; IQR	142; 66-203	145; 105-267	0.200
AFP			0.680
≤ 20	239 (47.8)	27 (43.5)	
> 20	261 (52.2)	35 (56.5)	
LS in kPa, median; IQR	10.8; 7.9-14.0	9.6; 8.0-12.3	0.150
SPA in cm ² , median; IQR	38.70; 38.50-41.10	39.16; 37.90-44.80	0.370
Tumor size in cm, median; IQR	3.1; 0.5-25.0	3.8; 0.7-13.0	0.230
Tumor number, median; IQR	1; 1.0-15.0	1; 1.0-2.0	0.090
RR			0.070
Minor	400 (80.0)	43 (69.4)	
Major	100 (20.0)	19 (30.6)	
BL in mL, median; IQR	100; 50-200	175; 50-300	0.390
Clamping time in min, median; IQR	15.0; 0-69	13.5; 0-60	0.150
HBV			0.570
Positive	468 (93.6)	60 (96.7)	
Negative	32 (6.4)	2 (3.3)	
HBV-DNA level			0.680
≥ 10 ³ IU/mL	286 (57.2)	32 (51.6)	
< 10 ³ IU/mL	32 (42.8)	30 (48.4)	
PHLF			0.250
Absent	358 (71.6)	40 (64.5)	
Present	142 (28.4)	22 (35.5)	
PHLF ISGLS grade			0.310
0-A	464 (92.8)	55 (88.7)	
B-C	36 (7.2)	7 (11.3)	

Data in parentheses were used to calculate percentages. AFP: Alpha-fetoprotein; ALB: Albumin; ALT: Alanine transaminase; BL: Blood loss; GGT: γ -

glutamyl transpeptidase; HB: Hemoglobin; HBV: Hepatitis B virus; INR: International normalized ratio, multiplied by 10; IQR: Interquartile range; ISGLS: International Study Group on Liver Surgery; LS: Liver stiffness; PHLF: Posthepatectomy liver failure; PLT: Platelet; PT: Prothrombin time; RR: Range of resection; SD: Standard deviation; SPA: Spleen area; TB: Total bilirubin; WBC: White blood cell.

Table 2 Comparison of model discrimination

Variables	Training cohort, n = 500			Validation cohort, n = 62		
	PM	ALBI	MELD	PM	ALBI	MELD
AUC (95%CI)	0.833 (0.792-0.873)	0.651 (0.598-0.703)	0.508 (0.436-0.548)	0.802 (0.684-0.920)	0.658 (0.536-0.774)	0.631 (0.499-0.750)
Sensitivity, %	83.100 (118/142)	43.700 (62/142)	62.000 (88/142)	95.500 (21/22)	72.300 (13/22)	59.100 (13/22)
Specificity, %	73.500 (263/358)	80.200 (287/358)	53.100 (190/358)	52.500 (21/40)	57.500 (29/40)	72.500 (29/40)
P value	-	< 0.001 ¹	< 0.001 ²	-	0.040 ³	0.048 ⁴

¹Area under receiver operating characteristic curve (AUC) values of the albumin-bilirubin (ALBI) score compared to that of the posthepatectomy liver failure model (PM) in the training cohort.

²AUC values of the model for end-stage liver disease (MELD) score compared to that of the PM in the training cohort.

³AUC values of the ALBI score compared to that of the PM in the validation cohort.

⁴AUC values of the model for end-stage liver disease score compared to that of the PM in the validation cohort.

CI: Confidence interval.

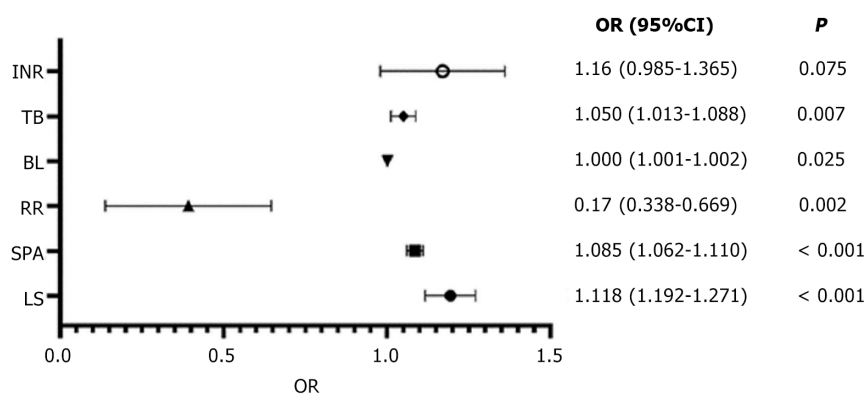


Figure 2 Forest plot of odds ratio for the multiple variables in logistic regression analysis. 95%CI: 95% confidence interval; BL: Blood loss; INR: International normalized ratio; LS: Liver stiffness OR: Odds ratio; RR: Resection range; SPA: Spleen area; TB: Total bilirubin.

inevitably lead to liver cell damage and decreased liver function. However, with the continuous refinement and standardization of surgical procedures, effective control of BL is not a complex and difficult task. By contrast, only a more accurate assessment of liver fibrosis/cirrhosis can predict liver reserve function more accurately, thereby improving the accuracy of predicting the occurrence of PHLF.

Ultrasound SWE has been confirmed and recommended by multiple guidelines for measuring LS to evaluate the degree of liver fibrosis[28-30], providing a theoretical basis for predicting PHLF by SWE-based LS measurement. Splenomegaly is associated with portal hypertension caused by cirrhosis and with poor prognosis[31,32]. Ultrasound is a convenient and useful tool for measuring spleen size.

In the prediction model we established, we found that LS and SPA measured by ultrasound were the independent risk factors for PHLF. Although many studies have established predictive models for PHLF based on LS measured by SWE in the past, the LS measured by SWE can be affected by inflammation. Indeed, there is often inflammation in HCC patients with liver fibrosis or even cirrhosis[33,34]. Therefore, considering the insufficient use of SWE alone to evaluate liver reserve function, a comprehensive evaluation of spleen size reflecting liver conditions was added. Bae *et al*[20] used specific software to measure spleen volume in three-dimensional computed tomography, and the results showed that spleen volume was an independent risk factor for predicting PHLF. However, their study required the use of unique software (Liver analysis, IntelliSpace Portal, Philips Health Systems), and the operation was time-consuming, which is not conducive to routine clinical use. The ultrasound measurement of spleen size in our study was simple and convenient, especially for patients with an enlarged spleen, making it more practical.

Previous studies have shown that PLT count was one of the risk factors for predicting PHLF[33], but our study did not show that PLT count was useful for predicting PHLF, which might be related to the criteria used when we included patients. For these thrombocytopenic patients, they were considered not eligible for surgery at our center. Therefore,

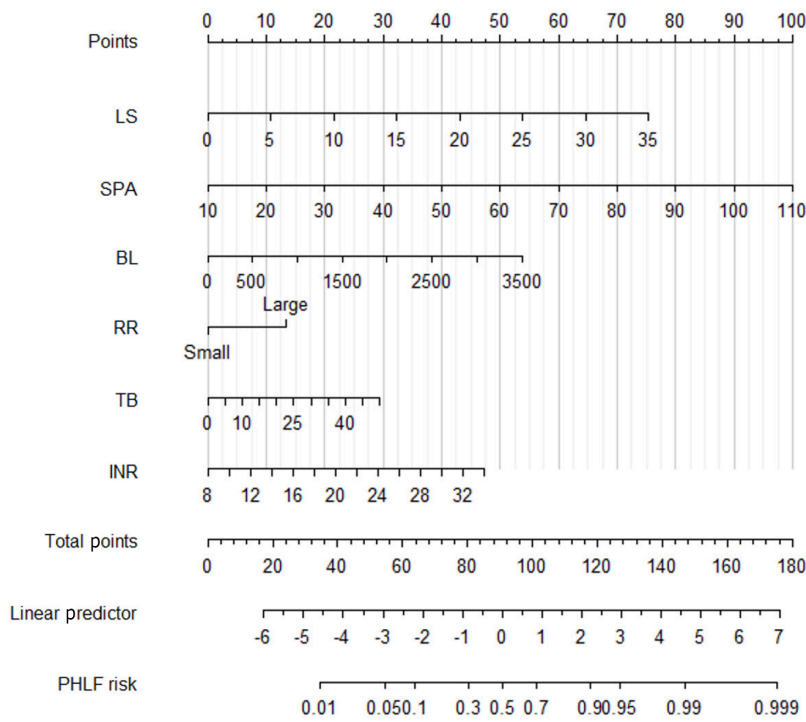


Figure 3 Nomogram of posthepatectomy liver failure model. BL: Blood loss; INR: International normalized ratio; LS: Liver stiffness; PHLF: Post-hepatectomy liver failure; RR: Resection range; SPA: Spleen area; TB: Total bilirubin.

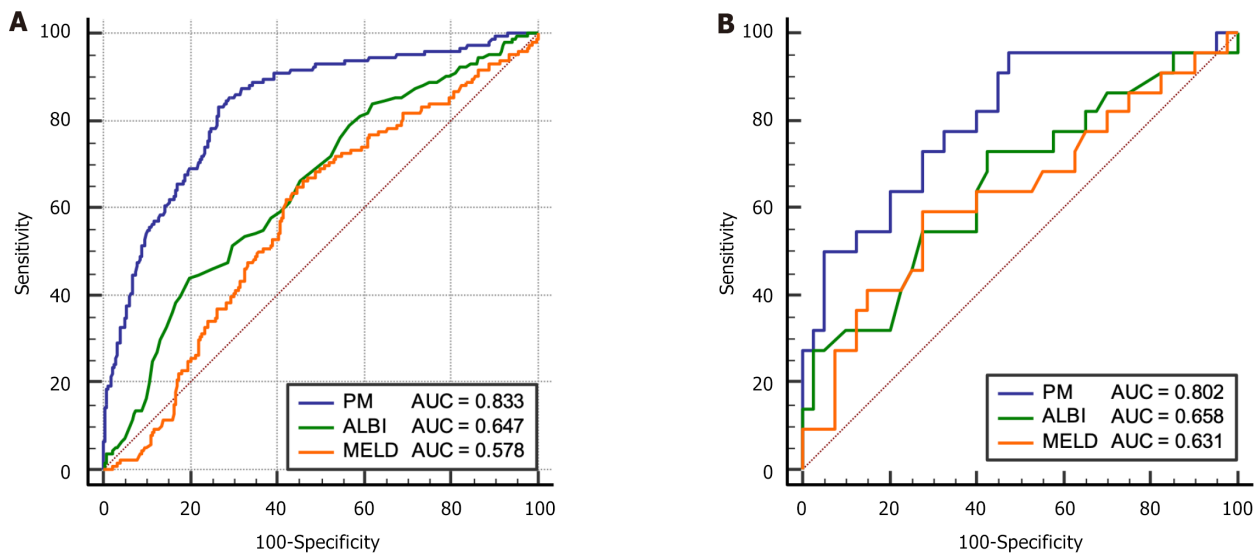


Figure 4 Receiver operating characteristic of models in training cohort and validation cohort. A: Training cohort; B: Validation cohort. ALBI: Albumin-bilirubin; MELD: Model of end-stage liver disease; PM: Posthepatectomy liver failure model.

many patients with severe thrombocytopenia were not included in this study.

We compared the established PM model with previous serological models ALBI and MELD in predicting liver failure, and the results showed that the PM model had a significantly higher AUC in predicting PHLF compared to ALBI and MELD. The sensitivity was always higher than the serological model, and the specificity was not always higher than the serological model. Since we hoped to effectively identify patients who might experience liver failure, we paid more attention to the sensitivity of the model in identifying liver failure. This model has achieved satisfactory sensitivity in both the training and validation cohort, and the AUC that reflected the diagnostic performance of the entire model was significantly better than the serological model.

We conducted a subgroup analysis of SPHLF and non-SPHLF. In the subgroup analysis, it was found that LS and RR were the independent risk factors of SPHLF, which seems understandable. Both RR and LS determine the number of effective liver cells in the residual liver after hepatectomy, thereby reflecting the liver reserve function of the residual liver after hepatectomy, which has been confirmed in previous studies[9,18,35]. We have determined that $LS \geq 12.52$ kPa is the

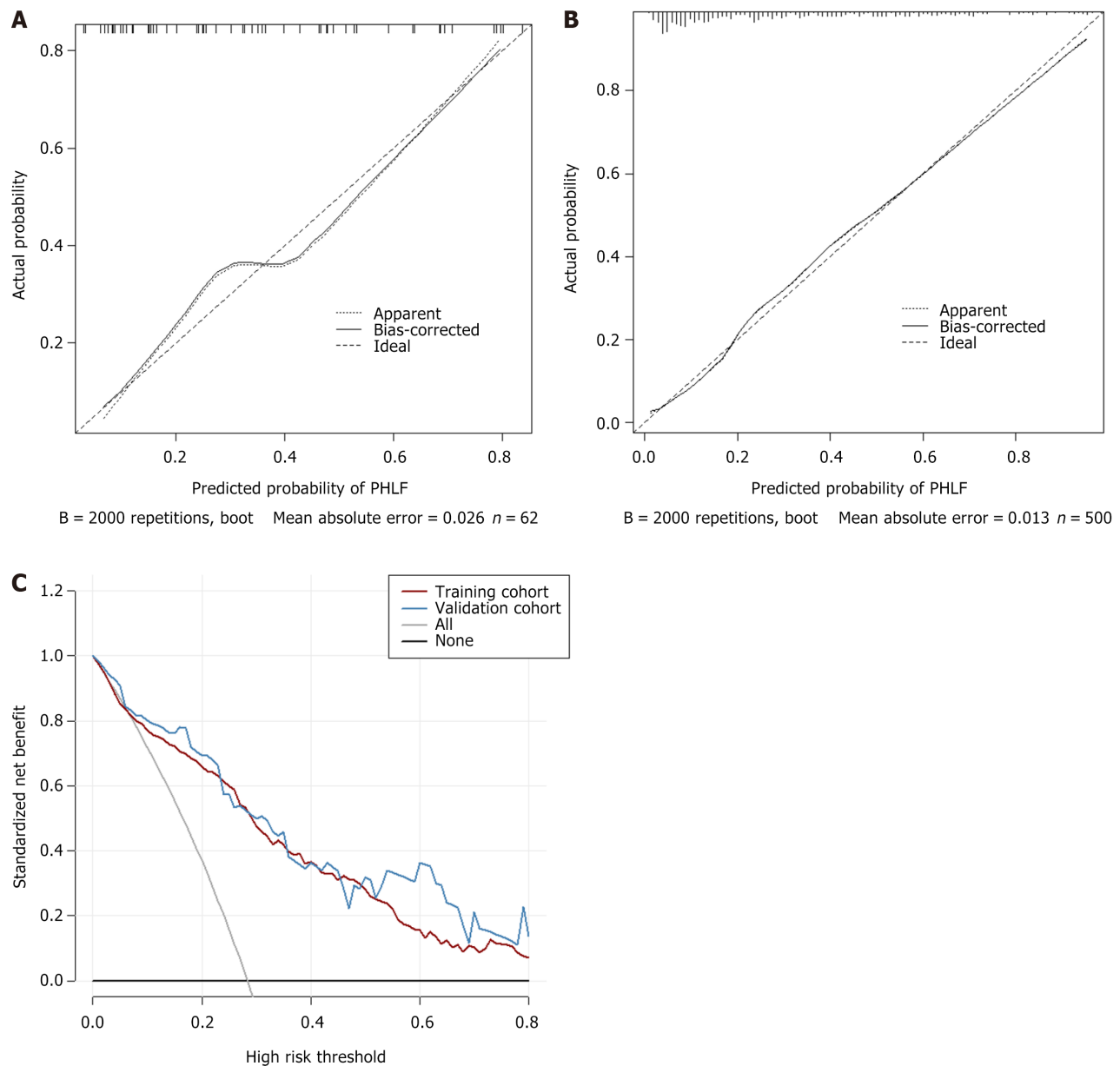


Figure 5 Figure calibration curves in the training cohort and the validation cohort and decision curve analysis of the prediction model. A: Training cohort; B: Validation cohort; C: Decision curve analysis of the prediction model. PHLF: Posthepatectomy liver failure.

cutoff value for diagnosing SPHLF. This is similar to the 11.90 kPa result obtained by Shen *et al*[34]. However, in the study of Long *et al*[18], the cutoff value for diagnosing SPHLF was 9.50 kPa and was quite different from our study, which might be related to the different number of cases and incidence rate of SPHLF between these studies. Namely, in the study by Long *et al*[18], 38 of 119 patients had SPHLF (an incidence rate of 31.9%), while in our study, 36 out of 500 patients had SPLF (an incidence rate of 7.2%). According to the new diagnostic criteria and literature, the incidence rate of PHLF is 9.0%-18.6%[36]. From the perspective of data, our incidence rate is closer to the literature reports, and our study was a multicenter study with a large sample size, better reflecting reality.

In addition, we conducted a subgroup analysis of the range of liver resection in the major liver resection group and the minor liver resection group. The results showed that the LS and SPA of PHLF patients in the major liver resection group were significantly lower than those in the minor liver resection group. In the case of a liver tumor with a large size that requires major liver resection, the LS greater than 10.34 kPa is recommended to prevent the occurrence of PHLF. However, when the tumor has a small range, the liver RR is also small, and the LS value reaches 13.48 kPa, we need to be alert to the occurrence of PHLF. Similarly, when the SPA is greater than 33.7 cm² and large liver resection is required, there may be a risk of PHLF. If minor liver resection is performed and the SPA reaches 43.2 cm² or more, there is a risk of PHLF.

The study had some limitations. First, almost the entire target population for this study included patients with HBV-related HCC, so this predictive nomogram needs further validation in patients with HCC of other etiologies, such as hepatitis C virus and alcohol abuse. Second, LS measurement by 2D-SWE reflects the stiffness of the focal liver tissue rather than that of the whole liver, which is an inherent limitation of ultrasound elastography. Third, the sample size in

the external validation cohort was not very large, so it is indispensable to increase the sample size for further external validation of the predictive nomogram.

CONCLUSION

In summary, our study established a nomogram for predicting the risk of developing PHLF by using data of patients from different centers. The nomogram showed better predictive performance than traditional models in both training and validation cohorts. In addition, the corresponding subgroup analysis for different situations provided surgeons with diagnostic cutoff values in different clinical scenarios, which can more effectively guide preoperative assessment of PHLF risk and effectively screen patients suitable for surgery.

ACKNOWLEDGEMENTS

We thank other centers involved in this multicenter study for their support in data collection.

FOOTNOTES

Author contributions: Cheng GW and Fang Y were responsible for designing the study, collecting data, analyzing data, and writing the paper. They contributed equally to this study. Xue LY, Zhang Y, Xie XY, Qiao XH, and Li XQ were responsible for the collection of cases and the collation of data. Ding H, Guo J and Xie XY were responsible for the authenticity and completeness of data from the center A and C, center B and D, and center E, respectively. All authors approved the final version of the manuscript for submission for publication. Ding H and Guo J contributed equally to this work as co-corresponding authors in responsibility for the design of the study, ethics, and overall research process, as well as for the writing and revision of the article.

Supported by the National Natural Science Foundations of China, No. 81873897 and No. 82102050; Shanghai Science and Technology Development Foundation, No. 22Y11911500; and Shanghai Municipal Health Commission of Science and Research Fund, No. 202140378.

Institutional review board statement: The study was reviewed and approved by the Medical Ethics Committee of Huashan Hospital of Fudan University (Approval No. 2020-1204).

Informed consent statement: All patients signed a presurgical informed consent form.

Conflict-of-interest statement: The authors declare that they have no competing interests.

Data sharing statement: The data underlying this article are available in HIMedc data manage system based on REDCap, at <http://www.himedc.cn> and requires authors' consent to be shared.

STROBE statement: The authors have read the STROBE Statement – checklist of items, and the manuscript was prepared and revised according to the STROBE Statement – checklist of items.

Open-Access: This article is an open-access article that was selected by an in-house editor and fully peer-reviewed by external reviewers. It is distributed in accordance with the Creative Commons Attribution NonCommercial (CC BY-NC 4.0) license, which permits others to distribute, remix, adapt, build upon this work non-commercially, and license their derivative works on different terms, provided the original work is properly cited and the use is non-commercial. See: <https://creativecommons.org/licenses/by-nc/4.0/>

Country of origin: China

ORCID number: Guang-Wen Cheng 0000-0002-8831-9213; Hong Ding 0000-0002-9998-0904.

S-Editor: Chen YL

L-Editor: Filipodia

P-Editor: Zhang XD

REFERENCES

- 1 **Sung H**, Ferlay J, Siegel RL, Laversanne M, Soerjomataram I, Jemal A, Bray F. Global Cancer Statistics 2020: GLOBOCAN Estimates of Incidence and Mortality Worldwide for 36 Cancers in 185 Countries. *CA Cancer J Clin* 2021; **71**: 209-249 [PMID: 33538338 DOI: 10.3322/caac.21660]
- 2 **Mullen JT**, Ribero D, Reddy SK, Donadon M, Zorzi D, Gautam S, Abdalla EK, Curley SA, Capussotti L, Clary BM, Vauthey JN. Hepatic insufficiency and mortality in 1,059 noncirrhotic patients undergoing major hepatectomy. *J Am Coll Surg* 2007; **204**: 854-62; discussion 862 [PMID: 17481498 DOI: 10.1016/j.jamcollsurg.2006.12.032]

- 3 **Shen YN**, Zheng ML, Guo CX, Bai XL, Pan Y, Yao WY, Liang TB. The role of imaging in prediction of post-hepatectomy liver failure. *Clin Imaging* 2018; **52**: 137-145 [PMID: 30059953 DOI: 10.1016/j.clinimag.2018.07.019]
- 4 **Noji T**, Uemura S, Wiggers JK, Tanaka K, Nakanishi Y, Asano T, Nakamura T, Tsuchikawa T, Okamura K, Olthof PB, Jarnagin WR, van Gulik TM, Hirano S. Validation study of postoperative liver failure and mortality risk scores after liver resection for perihilar cholangiocarcinoma. *Hepatobiliary Surg Nutr* 2022; **11**: 375-385 [PMID: 35693403 DOI: 10.21037/hbsn-20-660]
- 5 **El-Serag HB**. Epidemiology of viral hepatitis and hepatocellular carcinoma. *Gastroenterology* 2012; **142**: 1264-1273.e1 [PMID: 22537432 DOI: 10.1053/j.gastro.2011.12.061]
- 6 **Qiu T**, Fu R, Ling W, Li J, Song J, Wu Z, Shi Y, Zhou Y, Luo Y. Comparison between preoperative two-dimensional shear wave elastography and indocyanine green clearance test for prediction of post-hepatectomy liver failure. *Quant Imaging Med Surg* 2021; **11**: 1692-1700 [PMID: 33936957 DOI: 10.21037/qims-20-640]
- 7 **Rassam F**, Olthof PB, Bennink RJ, van Gulik TM. Current Modalities for the Assessment of Future Remnant Liver Function. *Visc Med* 2017; **33**: 442-448 [PMID: 29344518 DOI: 10.1159/000480385]
- 8 **Fu R**, Qiu T, Ling W, Lu Q, Luo Y. Comparison of preoperative two-dimensional shear wave elastography, indocyanine green clearance test and biomarkers for post hepatectomy liver failure prediction in patients with hepatocellular carcinoma. *BMC Gastroenterol* 2021; **21**: 142 [PMID: 33789567 DOI: 10.1186/s12876-021-01727-3]
- 9 **Xu B**, Li XL, Ye F, Zhu XD, Shen YH, Huang C, Zhou J, Fan J, Chen YJ, Sun HC. Development and Validation of a Nomogram Based on Perioperative Factors to Predict Post-hepatectomy Liver Failure. *J Clin Transl Hepatol* 2021; **9**: 291-300 [PMID: 34221915 DOI: 10.14218/JCTH.2021.00013]
- 10 **Luo N**, Huang X, Ji Y, Jin G, Qin Y, Xiang B, Su D, Tang W. A functional liver imaging score for preoperative prediction of liver failure after hepatocellular carcinoma resection. *Eur Radiol* 2022; **32**: 5623-5632 [PMID: 35294586 DOI: 10.1007/s00330-022-08656-z]
- 11 **Haimerl M**, Fuhrmann I, Poelsterl S, Fellner C, Nickel MD, Weigand K, Dahlke MH, Verloh N, Stroszczynski C, Wiggermann P. Gd-EOB-DTPA-enhanced T1 relaxometry for assessment of liver function determined by real-time (13)C-methacetin breath test. *Eur Radiol* 2018; **28**: 3591-3600 [PMID: 29532241 DOI: 10.1007/s00330-018-5337-y]
- 12 **Araki K**, Harimoto N, Kubo N, Watanabe A, Igarashi T, Tsukagoshi M, Ishii N, Tsushima Y, Shirabe K. Functional remnant liver volumetry using Gd-EOB-DTPA-enhanced magnetic resonance imaging (MRI) predicts post-hepatectomy liver failure in resection of more than one segment. *HPB (Oxford)* 2020; **22**: 318-327 [PMID: 31477460 DOI: 10.1016/j.hpb.2019.08.002]
- 13 **Gerber L**, Kasper D, Fitting D, Knop V, Vermehren A, Sprinzl K, Hansmann ML, Herrmann E, Bojunga J, Albert J, Sarrazin C, Zeuzem S, Friedrich-Rust M. Assessment of liver fibrosis with 2-D shear wave elastography in comparison to transient elastography and acoustic radiation force impulse imaging in patients with chronic liver disease. *Ultrasound Med Biol* 2015; **41**: 2350-2359 [PMID: 26116161 DOI: 10.1016/j.ultrasmedbio.2015.04.014]
- 14 **Bota S**, Paternostro R, Etschmaier A, Schwarzer R, Salzl P, Mandorfer M, Kienbacher C, Ferlitsch M, Reiberger T, Trauner M, Peck-Radosavljevic M, Ferlitsch A. Performance of 2-D shear wave elastography in liver fibrosis assessment compared with serologic tests and transient elastography in clinical routine. *Ultrasound Med Biol* 2015; **41**: 2340-2349 [PMID: 26004669 DOI: 10.1016/j.ultrasmedbio.2015.04.013]
- 15 **Zhuang Y**, Ding H, Zhang Y, Sun H, Xu C, Wang W. Two-dimensional Shear-Wave Elastography Performance in the Noninvasive Evaluation of Liver Fibrosis in Patients with Chronic Hepatitis B: Comparison with Serum Fibrosis Indexes. *Radiology* 2017; **283**: 873-882 [PMID: 27982760 DOI: 10.1148/radiol.2016160131]
- 16 **Shi Y**, Long H, Zhong X, Peng J, Su L, Duan Y, Ke W, Xie X, Lin M. The value of liver stiffness measured by two-dimensional shear wave elastography for predicting symptomatic posthepatectomy liver failure in patients with hepatocellular carcinoma. *Eur J Radiol* 2022; **150**: 110248 [PMID: 35299113 DOI: 10.1016/j.ejrad.2022.110248]
- 17 **Huang J**, Long H, Peng J, Zhong X, Shi Y, Xie X, Kuang M, Lin M. Predicting Post-hepatectomy Liver Failure Preoperatively for Child-Pugh A5 Hepatocellular Carcinoma Patients by Liver Stiffness. *J Gastrointest Surg* 2023; **27**: 1177-1187 [PMID: 36977863 DOI: 10.1007/s11605-023-05635-7]
- 18 **Long H**, Zhong X, Su L, Huang T, Duan Y, Ke W, Xie X, Lin M. Liver Stiffness Measured by Two-Dimensional Shear Wave Elastography for Predicting Symptomatic Post-hepatectomy Liver Failure in Patients with Hepatocellular Carcinoma. *Ann Surg Oncol* 2022; **29**: 327-336 [PMID: 34379248 DOI: 10.1245/s10434-021-10563-4]
- 19 **Kennedy P**, Wagner M, Castéra L, Hong CW, Johnson CL, Sirlin CB, Taouli B. Quantitative Elastography Methods in Liver Disease: Current Evidence and Future Directions. *Radiology* 2018; **286**: 738-763 [PMID: 29461949 DOI: 10.1148/radiol.2018170601]
- 20 **Bae JS**, Lee DH, Yoo J, Yi NJ, Lee KW, Suh KS, Kim H, Lee KB. Association between spleen volume and the post-hepatectomy liver failure and overall survival of patients with hepatocellular carcinoma after resection. *Eur Radiol* 2021; **31**: 2461-2471 [PMID: 33026503 DOI: 10.1007/s00330-020-07313-7]
- 21 **Peng W**, Zhang XY, Li C, Wen TF, Yan LN, Yang JY. Spleen stiffness and volume help to predict posthepatectomy liver failure in patients with hepatocellular carcinoma. *Medicine (Baltimore)* 2019; **98**: e15458 [PMID: 31045820 DOI: 10.1097/MD.00000000000015458]
- 22 **Oken MM**, Creech RH, Tormey DC, Horton J, Davis TE, McFadden ET, Carbone PP. Toxicity and response criteria of the Eastern Cooperative Oncology Group. *Am J Clin Oncol* 1982; **5**: 649-655 [PMID: 7165009]
- 23 **Chopinnet S**, Grégoire E, Bollon E, Hak JF, Palen A, Vidal V, Hardwigsen J, Le Treut YP. Short-term outcomes after major hepatic resection in patients with cirrhosis: a 75-case unicentric western experience. *HPB (Oxford)* 2019; **21**: 352-360 [PMID: 30120001 DOI: 10.1016/j.hpb.2018.07.020]
- 24 **Rahbari NN**, Garden OJ, Padbury R, Brooke-Smith M, Crawford M, Adam R, Koch M, Makuuchi M, Dematteeo RP, Christophi C, Banting S, Usatoff V, Nagino M, Maddern G, Hugh TJ, Vauthey JN, Greig P, Rees M, Yokoyama Y, Fan ST, Nimura Y, Figueras J, Capussotti L, Büchler MW, Weitz J. Posthepatectomy liver failure: a definition and grading by the International Study Group of Liver Surgery (ISGLS). *Surgery* 2011; **149**: 713-724 [PMID: 21236455 DOI: 10.1016/j.surg.2010.10.001]
- 25 **Prodeau M**, Drumez E, Duhamel A, Vibert E, Farges O, Lassailly G, Mabrut JY, Hardwigsen J, Régimbeau JM, Soubrane O, Adam R, Pruvot FR, Boleslawski E. An ordinal model to predict the risk of symptomatic liver failure in patients with cirrhosis undergoing hepatectomy. *J Hepatol* 2019; **71**: 920-929 [PMID: 31203152 DOI: 10.1016/j.jhep.2019.06.003]
- 26 **Rassam F**, Zhang T, Cieslak KP, Lavini C, Stoker J, Bennink RJ, van Gulik TM, van Vliet LJ, Runge JH, Vos FM. Comparison between dynamic gadoxetate-enhanced MRI and (99m)Tc-mebrofenin hepatobiliary scintigraphy with SPECT for quantitative assessment of liver function. *Eur Radiol* 2019; **29**: 5063-5072 [PMID: 30796575 DOI: 10.1007/s00330-019-06029-7]
- 27 **Fang T**, Long G, Wang D, Liu X, Xiao L, Mi X, Su W, Zhou L, Zhou L. A Nomogram Based on Preoperative Inflammatory Indices and ICG-

- R15 for Prediction of Liver Failure After Hepatectomy in HCC Patients. *Front Oncol* 2021; **11**: 667496 [PMID: 34277414 DOI: 10.3389/fonc.2021.667496]
- 28 **European Association for Study of Liver**; Asociacion Latinoamericana para el Estudio del Hgado. EASL-ALEH Clinical Practice Guidelines: Non-invasive tests for evaluation of liver disease severity and prognosis. *J Hepatol* 2015; **63**: 237-264 [PMID: 25911335 DOI: 10.1016/j.jhep.2015.04.006]
- 29 **Barr RG**, Wilson SR, Rubens D, Garcia-Tsao G, Ferraioli G. Update to the Society of Radiologists in Ultrasound Liver Elastography Consensus Statement. *Radiology* 2020; **296**: 263-274 [PMID: 32515681 DOI: 10.1148/radiol.2020192437]
- 30 **Ferraioli G**, Wong VW, Castera L, Berzigotti A, Sporea I, Dietrich CF, Choi BI, Wilson SR, Kudo M, Barr RG. Liver Ultrasound Elastography: An Update to the World Federation for Ultrasound in Medicine and Biology Guidelines and Recommendations. *Ultrasound Med Biol* 2018; **44**: 2419-2440 [PMID: 30209008 DOI: 10.1016/j.ultrasmedbio.2018.07.008]
- 31 **Yoshida H**, Shimizu T, Yoshioka M, Matsushita A, Kawano Y, Ueda J, Kawashima M, Taniai N, Mamada Y. The Role of the Spleen in Portal Hypertension. *J Nippon Med Sch* 2023; **90**: 20-25 [PMID: 36908126 DOI: 10.1272/jnms.JNMS.2023_90-104]
- 32 **Patel M**, Tann M, Liangpunsakul S. CT-scan Based Liver and Spleen Volume Measurement as a Prognostic Indicator for Patients with Cirrhosis. *Am J Med Sci* 2021; **362**: 252-259 [PMID: 33947583 DOI: 10.1016/j.amjms.2020.10.031]
- 33 **Hu H**, Han H, Han XK, Wang WP, Ding H. Nomogram for individualised prediction of liver failure risk after hepatectomy in patients with resectable hepatocellular carcinoma: the evidence from ultrasound data. *Eur Radiol* 2018; **28**: 877-885 [PMID: 28779402 DOI: 10.1007/s00330-017-4900-2]
- 34 **Shen Y**, Zhou C, Zhu G, Shi G, Zhu X, Huang C, Zhou J, Fan J, Ding H, Ren N, Sun HC. Liver Stiffness Assessed by Shear Wave Elastography Predicts Postoperative Liver Failure in Patients with Hepatocellular Carcinoma. *J Gastrointest Surg* 2017; **21**: 1471-1479 [PMID: 28510795 DOI: 10.1007/s11605-017-3443-9]
- 35 **Shimada S**, Kamiyama T, Kakisaka T, Orimo T, Nagatsu A, Asahi Y, Sakamoto Y, Kamachi H, Kudo Y, Nishida M, Taketomi A. The impact of elastography with virtual touch quantification of future remnant liver before major hepatectomy. *Quant Imaging Med Surg* 2021; **11**: 2572-2585 [PMID: 34079724 DOI: 10.21037/qims-20-1073]
- 36 **Skrzypczyk C**, Truant S, Duhamel A, Langlois C, Boleslawski E, Koriche D, Hebbar M, Fourrier F, Mathurin P, Pruvot FR. Relevance of the ISGLS definition of posthepatectomy liver failure in early prediction of poor outcome after liver resection: study on 680 hepatectomies. *Ann Surg* 2014; **260**: 865-70; discussion 870 [PMID: 25243550 DOI: 10.1097/SLA.0000000000000944]



Published by **Baishideng Publishing Group Inc**
7041 Koll Center Parkway, Suite 160, Pleasanton, CA 94566, USA
Telephone: +1-925-3991568
E-mail: office@baishideng.com
Help Desk: <https://www.f6publishing.com/helpdesk>
<https://www.wjgnet.com>

